Available online at www.sciencedirect.com
SCIENCE DIRECT®
Materials Chemistry and Physics 89 (2005) 38–48
MATERIALS CHEMISTRY AND PHYSICS
www.elsevier.com/locate/matchemphys

Effect of some thiophene derivatives on the electrochemical behavior of AISI 316 austenitic stainless steel in acidic solutions containing chloride ions
I. Molecular structure and inhibition efficiency relationship

A. Galal*, N.F. Atta, M.H.S. Al-Hassan

Department of Chemistry, College of Science, University of Cairo, Giza, Egypt

Received 4 July 2004; received in revised form 10 August 2004; accepted 24 August 2004

Abstract

The electrochemical behavior of austenitic stainless steel (AISI 316) was studied in an acid medium that contains chloride ions in absence and presence of some thiophene derivatives. The corrosion rate as well as pit growth of the steel was inhibited variably with each of the sulfur-containing compound present in the corroding medium. The thiophene derivatives studied were 2-acetyl thiophene (AcT), 2-thiophene carboxylic acid (TCA), 3-thiophene carboxyaldehyde (TCAL) and 2-thiophene carboxylic hydrazide (TCH). Electrochemical techniques such as potentiodynamic polarization, Tafel experiments, polarization resistance and electrochemical impedance spectroscopy were used to investigate the electrochemical behavior of the steel. The results showed distinct effects for the different thiophene derivatives used that depended on the molecular structure and the electron density of the sulfur atom of the thiophene ring. The order of inhibition efficiency was TCH > TCA > TCAL > AcT. It was also concluded that the inhibitors studied were of the mixed type. This conclusion was realized by comparing the change in the values of the anodic and cathodic Tafel slopes. Inhibition efficiencies of ca. 97% were achieved using these inhibitors in 0.5 M H_2SO_4.

Keywords: Electrochemistry; Corrosion; Stainless steel; Thiophene derivatives; Molecular structure

1. Introduction

Stainless steels have technological and economic importance [1]. They are iron alloys containing a minimum of approximately 11% chromium. This amount of chromium prevents the formation of rust in “unpolluted” atmospheric environments [2]. Nowadays, there are more than 190 different kinds of alloys that can be recognized as belonging to the stainless steel family. Stainless steels are used in a wide variety of services in which primary considerations are long service life (in a given environmental condition), reliability, appearance and sanitary factors. Recent interest is the use of these materials in the medical field [3]. Moreover, the corrosion rate of “reactive” metals and alloys can be suppressed to a great extent by modification of the metal surface by organic molecules or polymers.

In this respect, organic inhibitors are well known to affect the rate of metallic corrosion by decreasing the rate of either or both the anodic metal dissolution and the cathodic oxygen reduction [4]. The inhibition mechanism is generally affected by the chemical changes occurring to the inhibitor and changes to the electrolytic medium. The general possible scenarios are: (i) partial or (ii) full dissolution of the inhibitor, or (iii) its adsorption at the metal surface. For example, hydrazinium reduces the oxygen activity and adsorb at the metal/electrolyte interface. The adsorption of hydrazinium at the metal/electrolyte interface leads to the enhancement of passive film formation as in the case of benzotriazol adsorption at the copper surface and benzoates on

* Corresponding author. Tel.: +20 2 782 5266; fax: +20 2 568 5799.
E-mail address: galalah1@yahoo.com (A. Galal).

0254-0584/$ – see front matter © 2004 Elsevier B.V. All rights reserved.
doi:10.1016/j.matchemphys.2004.08.019

iron surfaces [5]. On the other hand, monomolecular adsorption layers of inhibitors, known as interfacial inhibitors [6], prevent the dissolution of the substrate and the reduction of oxygen by changing the potential drop across the interface and/or the reaction mechanism thereafter.

The inhibition characteristics of some inhibitors during acid corrosion have been reported earlier [7–14]. The protection efficiency was attributed mainly to the presence of a polar atom or more such as nitrogen, sulfur and oxygen in the inhibiting molecule. N, S, and O atoms act as active centers for adsorption of the organic molecule onto the metallic surfaces. The inhibiting effect of molybdate and chromate ions on the pitting corrosion of AISI 304 and 316 steels were studied in acid medium and the results presented show that these known inhibitors affect both the nucleation of pitting and metastable pitting by reducing the numbers and sizes of these events [15]. Several organic compounds were evaluated as inhibitors for the corrosion of AISI 304 stainless steel in acid medium [16–19].

Marawi et al. [20], as well as others [21], investigated the formation of polymeric conductive layers over "active" metallic substrates. In this study, an interaction was found between the sulfur atom of the repeat unit forming the polymer layer of the thiophene-based structure and the steel substrate. This interaction was the base that led to the full nucleation of the polymer over the substrate surface. There is almost no mention in the literature of the electrochemistry of thiophene-based molecules at stainless steels surfaces. Moreover, the electrochemical behavior and inhibiting effect of 3-methylthiophene was not previously mentioned in the literature. The empty electronic bands of the solid substrate, predominantly iron in this case, overlap with pair of electrons of the adsorbed molecules namely. The electron transfer process between the molecule and the substrate is characteristic for transition metals having vacant low-energy d-electron orbital.

The aim of the present work was to investigate the electrochemical behavior of stainless steel of type AISI 316 in acid medium containing chloride in presence and absence of some thiophene derivatives. Also, to correlate the inhibition efficiency of the inhibitors studied to their geometrical structures and nature of substituent in the hetero-ring, and to determine the morphological changes of the surface before and after treatment in the corroding medium.

2. Experimental details

2.1. Materials and preparations

AISI 316 stainless steel was used in this study, with the following chemical composition (in wt.%): 16.9 Cr, 10.9 Ni, 75 Si, 1.24 Mn, 0.025 N, 0.027 S, 0.20 Cu, 2.11 Mo, 0.053 C, Fe (balance). Stainless steel samples were purchased from Goodfellow (Huntingdon, England).

Sulfuric acid, sodium chloride, 2-thiophene carboxylic hydrazide (TCH), 2-thiophene carboxylic acid (TCA), 3-thiophene carboxaldhyde (TCAL), and 2-acetyl thiophene (AcT) were purchased from Aldrich (Wisconsin, USA) and were used as received. The structure and some properties of the inhibitors used in this study are shown in Fig. 1.

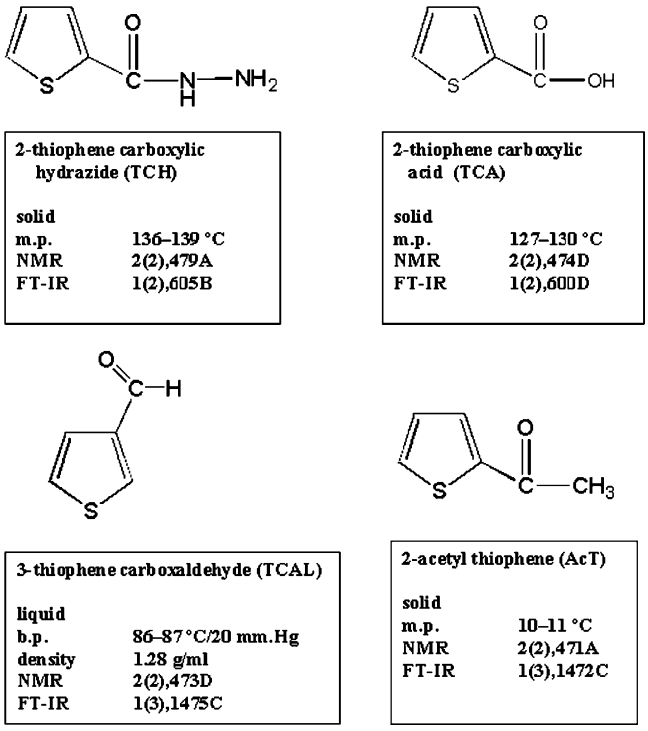

Fig. 1. Structure and some properties of the thiophene derivatives.

Test solutions were prepared from stock and diluted using de-ionized water supply. Water was first distilled and then de-ionized using a Millipore water purification system. Different concentrations of the inhibitor were prepared by dilution of the 0.1 M stock solution of the inhibitor, and then diluted by the test solution (H_2SO_4 in presence or absence of chloride ions) to the appropriate concentration (between 5×10^{-4} and 1×10^{-2} M). It is important to mention that TCA, TCAL and AcT were dissolved in 1% ethanol/H_2SO_4 when preparing their respective stock solutions.

2.2. Electrode mounting and electrochemical cell

The steel specimens were in the form of rods. The specimens were prepared and mounted according to the following steps. The stainless steel rods were cut in the dimensions of 20 mm long and 6 mm diameter. The specimen was then grooved and threaded for electrical contact and connection. A copper rod 120 mm long and 3.5 mm diameter was used for establishing the electrical contact. The whole assembly was inserted in a glass tube 100 mm long and 8 mm i.d. Epoxy resin (Torr^{TM} Seal, from Varian, MI, USA) was used to ensure the exposure of a determined apparent surface area of 0.283 cm^2. The electrode surface was polished mechanically using metallurgical papers of successive grades (120, 600 and 1200 μm), further surface polishing using alumina paste

0.3 μm dispersed on a soft cloth paper was pursued until a scratch-free surface is obtained. The electrode was rinsed with distilled water, degreased in ethanol and was thoroughly rinsed with de-ionized water.

A three-electrode one-compartment glass cell, with a saturated Ag/AgCl reference electrode and a platinum sheet (2 cm × 2 cm) counter electrode was used for all the electrochemical measurements.

2.3. Electrochemical equipments and measurements

A Gamry PC3/750 potentiostat/galvanostat/ZRA system (Gamry Inc., USA) was used for potential-controlled polarization measurements. This system was interfaced to a personal computer to control the experiments were controlled and the data were analyzed using a Gamry framework/analysis software. Potentiodynamic polarization measurements were carried out on the stainless steel electrode in 0.5 M H_2SO_4 in presence and absence of each inhibitor. Tafel plots and polarization resistance measurements were conducted after the electrode potential reaches a steady-state value of ±2 mV that usually takes ca. 15 min after immersion in the test solution. Potentiodynamic polarization, Tafel, and polarization resistance measurements conditions are as follows: $E_i = -1.0$ V, $E_f = +1.5$ V (versus $E_{reference}$), scan rate = 5 mV s^{-1}; $E_i = -250$ mV, $E_f = +250$ mV (versus E_{corr}), scan rate = 1 mV s^{-1}; and $E_i = -20$ mV, $E_f = +20$ mV (versus E_{corr}), scan rate = 0.1 mV s^{-1}, respectively. Electrochemical impedance spectroscopy (EIS) experiments were performed on stainless steel samples in presence and absence of inhibitor at constant applied potential. The experimental conditions were as follows: frequency range between 0.020 Hz and 5.0 kHz, two constant applied potential values were used (ca. −100 and +200 mV versus E_{corr}) and a small alternating current (AC) perturbation signal of 10 mV was superimposed to the direct current (DC) signal. Data analysis and interpretation were treated according to the methods described earlier in the literature [22,23]. All electrochemical measurements were performed at room temperature (ca. 20 ± 0.2 °C).

3. Results and discussion

3.1. Potentiodynamic behavior

This part of the present work investigates the electrochemical behavior of stainless steel electrode in the absence/presence of different concentrations of the above thiophene compounds in acidic and chloride-containing acidic solutions. Potentiodynamic polarization experiments of AISI 316 stainless steel in 1.0 M H_2SO_4 at 25 °C in absence (a) and presence (b) of TCH is shown in Fig. 2. The following observations could be withdrawn from the data:

- The general shape of the potentiodynamic curve in the absence and presence of the inhibitor is comparable. However, the linear parts of anodic and cathodic Tafel regions appeared extended over wider current range in the presence of the inhibitor when compared to that in the absence of the inhibitor.
- The calculated corrosion potential, E_{corr}, in the case of the curve (b) in presence of the inhibitor is −299.2 mV with an associated corrosion current, i_{corr}, of 7.37×10^{-5} A cm^{-2}. The corresponding values in the absence of the inhibitor are −1.0 mV and 1.385×10^{-3} A cm^{-2}, respectively. The comparison of the values of E_{corr} and i_{corr} indicated that the addition of 1.0×10^{-2} M TCH resulted in the shift of the corrosion potential to a negative value and an appreciable decrease in the corrosion current density, ca. two orders of magnitudes.
- The comparison of the values of the anodic and cathodic Tafel constants, β_a, β_c, resulted in distinct values of 153.7 and 145.0 mV $decade^{-1}$ and 46.4 and 86.0 mV $decade^{-1}$ in absence and presence of the inhibitor, respectively. Thus, it is concluded that the inhibitor appeared to be of the mixed type. On one hand, the rate of hydrogen evolution is

$$2H^+ + 2e^- \rightarrow 2H \rightarrow H_2$$

is altered by the adsorbed layer thus formed due to the presence of the organic inhibitor. On the other hand, the tendency of these thiophene-based molecules to adsorb at the electrode surface limit the diffusion of oxygen to the surface and trap the metal ions on the surface that results in reducing the rate of dissolution and helps in producing a passive film in the anodic part of the potentiodynamic

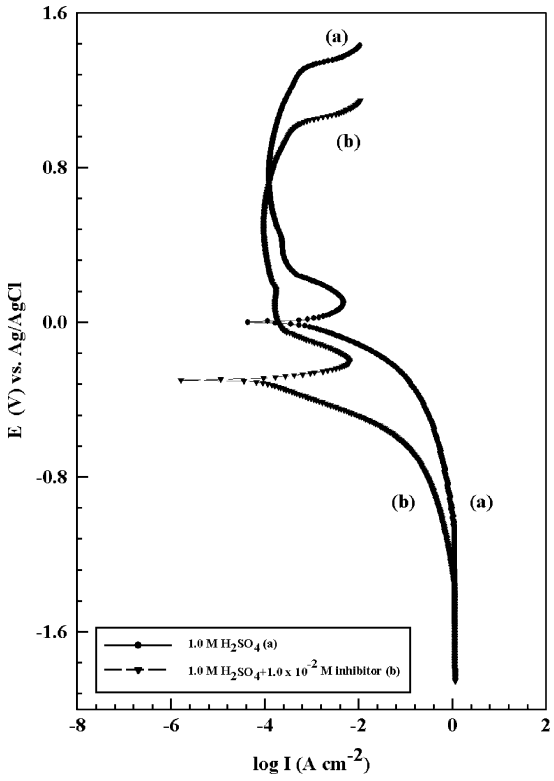

Fig. 2. Potentiodynamic polarization experiments of AISI 316 stainless steel in 1.0 M H_2SO_4 at 25 °C in absence (a) and presence (b) of TCH.

curve [24]. Moreover, a dissolution/precipitation mechanism cannot be excluded as the β_a value approaches the theoretical value, ca. 40 mV decade^{-1}, suggested by Bockris and Drasic [25].

- The potentiodynamic curve was characterized by the appearance of a well-defined anodic peak that appeared at +108.1 mV, which corresponds to an anodic peak current of 6.21×10^{-3} A cm^{-2} in absence of the inhibitor. On the other hand, the corresponding values in presence of TCH are -200.5 mV and 7.8×10^{-3} A cm^{-2}, respectively.
- The anodic peak in both curves was followed by a slight increase in the current value and finally an almost constant value. In spite of the increase in current, oxygen evolution was not noticed by the naked eye as the potential exceeded the value of 1.0 V versus Ag/AgCl. Thereafter, an ill-defined peak is observed in the active–passive region.
- The polarization resistance values, calculated from the potentiodynamic curve were 2.340×10^1 and 1.777×10^2 Ω cm^2 for the non-inhibited solution and the inhibited one, respectively. The corresponding calculated corrosion rates are 1.283×10^3 and 6.755×10^1 MPY (milli-inch per year = 0.00219 mA cm^{-2}), respectively, that resulted in lowering of ca. 94.7% in the rate of corrosion of the inhibited stainless steel in the 1.0 M H_2SO_4 solution.

3.2. Effect of chloride ions

Sodium chloride with concentration of 0.01 M was added to the acidic solution to form a concentration ratio of H_2SO_4/NaCl of 10/1. The following treatment of the results is based on comparing the results obtained from the potentiodynamic experiments of the stainless steel in presence and absence of 1.0×10^{-2} M TCH. Thus, potentiodynamic polarization experiments of stainless steel in 0.01 M NaCl/0.1 M H_2SO_4 at 25 °C in absence (a) and presence (b) of 1.0×10^{-2} M TCH are shown in Fig. 3. The following observations could be withdrawn from the data:

- The general shape of the potentiodynamic curves in the absence and presence of the inhibitor are comparable to those obtained in Fig. 2 for stainless steel tested in 1.0 M H_2SO_4.
- The linear anodic and cathodic Tafel regions are apparently the same as shown in Fig. 3a and b, respectively. The anodic and cathodic parts of the Tafel region in presence of TCH showed, however, extended linear region when compared to the non-inhibited solution.
- The calculated corrosion potential, E_{corr}, in the case of the curve b in presence of the inhibitor is -375.3 mV with an associated corrosion current, i_{corr}, of 2.820×10^{-5} A cm^{-2}. The corresponding values in the absence of the inhibitor are -332.1 mV and 2.068×10^{-4} A cm^{-2}, respectively. The comparison of the values of E_{corr} and i_{corr} indicated that the addition of TCH resulted in a "cathodic" shift in the corrosion potential values as compared to the study made in 1.0 M H_2SO_4. Moreover, a decrease in the corrosion current density is still noticed with an appreciable decrease by ca. 1 decade. The later resulted in a noticeable decrease in the corrosion rate from 189.56 to 25.85 MPY and an inhibition efficiency of 86.4%. The relative decrease in the protection efficiency in this case when compared to the aforementioned values for the inhibitor in the pure acidic medium, could be explained in terms of the initiation of pitting nucleation in the anodic part of the polarization curve and the possible adsorption hindrance suffered by the TCH in presence of solvated chloride ions. Actually, visual examination of the electrode surface after the polarization experiment revealed observable pits.
- Tafel slopes, β_c and β_a, for the cathodic and anodic processes exhibited lower values upon the addition of TCH, namely, 83.4/65.7 mV decade^{-1} in presence as compared to 119.5/82.0 mV decade^{-1} in absence of inhibitor. The values are relatively lower than those cited in the literature for stainless steel of type AISI 304 [14].

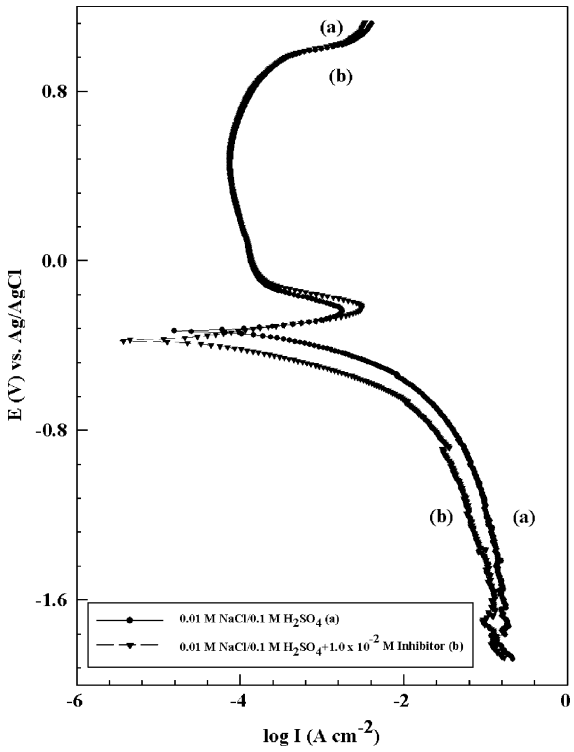

Fig. 3. Potentiodynamic polarization experiments of stainless steel in 0.01 M NaCl/0.1 M H_2SO_4 at 25 °C in absence (a) and presence (b) of 1.0×10^{-2} M TCH.

3.3. Effect of varying the inhibitor concentration

The effect of varying the concentration of the inhibitor with fixed concentration of sulfuric acid, ca. 0.5 M, on the corrosion of the AISI 316 steel was examined in this section for two thiophene derivatives. The data for these experiments are summarized in tables in presence/absence of TCAL and AcT at room temperature (25 °C), respectively. The following observations could be withdrawn when comparing the data:

- The potentiodynamic curves (not shown) exhibited distinct features when changing the type of inhibitor used. Thus, as the concentration of TCAL increases in the medium the corrosion potential, E_{corr}, shifted to relatively more cathodic values. On the other hand, the corrosion potential remained basically constant in the case of using AcT.
- An anodic peak is observed immediately after the extended anodic Tafel line for which the corresponding peak current and peak potential values changed upon changing the concentration of the inhibitor. In general, the peak current values shifted to lower values and that of the peak potential values shifted to relatively more positive values. These effects were more pronounced in the case of using TCAL.
- The inhibition efficiency increased as the concentration of the inhibitor increases. This is clearly shown when examining the values of the polarization resistance, R_p, and the corresponding corrosion rates calculated as shown in Table 1a and b, respectively. However, the inhibition efficiency for TCAL is higher than that of AcT.
- Again, it is important to notice that unexpectedly the values of the Tafel constants (β_a and β_c), namely the anodic slopes, are relatively lower than those cited in the literature [14]. Moreover, the addition of the inhibitor to the medium changed both values of β_a and β_c. This indicates that these two inhibitors are also of the mixed types as mentioned earlier in this section.

The potentiodynamic anodic plot is practically useful to determine important information such as: (i) the ability of the material to spontaneously passivate in the particular medium, (ii) the potential region over which the specimen remains passive, and (iii) the corrosion rate in the passive region. Anodic and cathodic Tafel slopes are used to calculate the corrosion rate using the linear polarization method according to:

$$\eta = \beta \log \frac{i}{i_{corr}} \tag{1}$$

where η is the overvoltage, or the difference between the potential of the specimen and the corrosion potential, β the Tafel constant (slope) and i_{corr} the current at overvoltage η. Rearranging Eq. (1) gives

$$\eta = \beta(\log i - \log i_{corr}) \tag{2}$$

A plot of η versus $\log i$ is a straight line with slope β. As could be noticed from Eq. (2), when $\eta = 0$ (at E_{corr}), $\log i/i_{corr} = 0$, $i/i_{corr} = 1$, and $i = i_{corr}$. The anodic and cathodic Tafel constants are used to calculate the corrosion rate from polarization measurement data according to the following equation [26]:

$$\frac{\Delta E}{\Delta i} = \frac{\beta_a \beta_c}{2.3(i_{corr})(\beta_a \beta_c)} \tag{3}$$

where $\Delta E/\Delta i$ is the slope of the polarization resistance plot (ΔE expressed in V and Δi expressed in μA). The values of the Tafel constants are determined from the Tafel plot, i_{corr} being the corrosion current in μA. Rearranging Eq. (3) yields:

$$i_{corr} = \frac{\beta_a \beta_c}{2.3 i_{corr} \beta_a \beta_c} \frac{\Delta i}{\Delta E} \tag{4}$$

Therefore, the corrosion current can be related directly to the corrosion rate (r) by the following equation:

$$r\,(\mathrm{MPY}) = \frac{0.13\, i_{corr}(\mathrm{EW})}{d} \tag{5}$$

EW is the equivalent weight of the corroding species, d the density of the corroding species and i_{corr} the corrosion current density. The inhibition efficiency (p) is given by the following relation:

$$p = \left[\frac{i_{corr(un)} - i_{corr(inh)}}{i_{corr(un)}} \right] \times 100 \tag{6}$$

$i_{corr(un)}$ and $i_{corr(inh)}$ are the measured corrosion currents in absence and presence of inhibitor, respectively.

3.4. Effect of varying the concentration of sulfuric acid on the efficiency of inhibition

Polarization data for inhibited and uninhibited stainless steel 316 in 0.1, 0.5, and 1.0 M sulfuric acid solutions are given in Table 2. Anodic and cathodic Tafel slopes were reported earlier in the range β_a/β_c = 121/87.5−169/106 [27,28]. A noticeable difference is clearly observed in this study that indicates a change in the mechanism of inhibition for the thiophene derivatives when compared to those investigated previously. As mentioned in preceding section, the thiophene derivatives (TCAL and AcT) appeared to act as mixed inhibitors. This observation was again proved when comparing the values of the anodic and cathodic Tafel constants (β_a/β_c) in the case of applying TCH (cf. Table 2). The values in different concentrations of H_2SO_4 ca. 0.1, 0.5, and 1.0 M are: 58/106, 55/88, and 145/154 mV decade^{-1}, in absence of TCH. The corresponding values in presence of 1.0×10^{-2} M TCH are 89/77, 39/7, and 86/46 mV decade^{-1}, respectively.

Two observations are worthwhile mentioning: First, the values of the cathodic Tafel constant, β_c, calculated for inhibited solutions are smaller than those obtained for the unin-

Table 1
Electrochemical parameters for stainless steel 316 in 0.5 M H_2SO_4 in absence and presence of 3-thiophene carboxaldehyde (TCAL)/2-acetyl thiophene (AcT)

Inhibitor (mol l^{-1})	E (mV)		β_c (mV decade^{-1})	β_a (mV decade^{-1})	R_p (10^2 Ω cm^2)	I_{corr} (10^{-4} A cm^{-2})	Corrosion rate (MPY)
	E_{oc}	E_{cor}					
0	−328/−328	−348/−348	88/88	55/55	1.64/1.64	0.90/0.90	82.5/82.5
5×10^{-4}	−362/−371	−354/−355	113/76	31/56	3.95/4.34	0.27/0.32	24.4/29.7
1×10^{-2}	−378/−382	−364/−373	79/71	100/77	27.0/19.8	0.058/0.080	4.5/7.4

Table 2
Electrochemical parameters for stainless steel type 316 in different concentrations of H_2SO_4 in absence and presence of 1.0×10^{-2} M 2-thiophene carboxylic hydrazide (TCH)

Electrolyte (mol l^{-1})	E (mV)		β_c (mV decade^{-1})	β_a (mV decade^{-1})	R_p (10^2 Ω cm^2)	I_{corr} (10^{-4} A cm^{-2})	Corrosion rate (MPY)
	E_{oc}	E_{cor}					
0.1 M H_2SO_4	−352	−349	106	58	4.57	0.36	33.2
0.1 M H_2SO_4 +10^{-2} M TCH	−394	−404	77	89	5.39	0.033	23.1
0.5 M H_2SO_4	−328	−348	88	55	1.64	0.90	82.5
0.5 M H_2SO_4 +10^{-2} M TCH	−315	−329	79	39	32.4	0.059	3.40
1.0 M H_2SO_4	−16	−1.0	154	145	0.234	14	1280
1.0 M H_2SO_4 +10^{-2} M TCH	−309	−299	46	86	1.77	0.74	68.3

hibited ones in all H_2SO_4 concentrations studied. On the other hand, with the exception for 0.5 M H_2SO_4, the values of the anodic Tafel constant, β_a, showed an opposite trend. Second, the polarization resistance values calculated from the potentiodynamic curve were 4.56/5.39 × 10^2, 1.64/32.4 × 10^2, 0.234/1.78 × 10^2 Ω cm^{-2} for the uninhibited/inhibited solutions with different concentrations of H_2SO_4, respectively. The corresponding calculated corrosion rates are 33.16/3.07, 82.54/3.40, and 1283/68.26 MPY, respectively. Again, a reduction of up to about 94.7% in the rate of corrosion of the inhibited stainless steel in the 1.0 M H_2SO_4 is, therefore, observed when compared to the non-inhibited one. The corrosion rate observed in the more concentrated solution was, however, relatively higher than those found in the less concentrated acid solution. An exception was observed in the case of H_2SO_4 with a concentration of 0.5 M, in which the stainless steel surface exhibited a peculiar trend. Thus, in the uninhibited solution, the electrode did not show a passive peak current when compared to the electrode examined in the 0.1 and 1.0 M solutions, respectively. However, the presence of the inhibitor led to the formation of a passive peak in all concentrations. At this stage the value of corrosion rate in presence of TCH in 0.5 M H_2SO_4 cannot be compared to the uninhibited solution. This concentration of sulfuric acid, ca. 0.5 M, is critical to the formation of the passive layer that appeared to be destabilized at the surface [29].

Examination of the surface of the stainless steel electrode after exposure to different concentrations of sulfuric acid solutions (0.1, 0.5 and 1.0 M) did not show eye-detectable pitting. However, the solution became reddish-brown in color after the polarization experiment. A detailed description of the surface morphology of the electrode will be given in a separate paper [30].

3.5. Effect of the molecular structure on the efficiency of thiophene inhibitors

The relationship between the structure of the inhibitor molecule and its inhibiting efficiency has been the subject of several investigations [28,31–33]. However, much less attention has been paid to the dependence of the inhibition efficiency on the size and electronic distribution in the inhibitor molecule at the stainless steel surfaces. In this part of the present investigation, we will attempt to answer the following questions:

(a) What is the effect of changing the functional group in the side chain of the thiophene derivative on the percent inhibition efficiency?
(b) What is the relation between the structure of the inhibitor molecules studied and their inhibition efficiencies?
(c) What is the effect of changing the inhibitor on the mechanism of corrosion?

Energy minimization was used in order to display the compounds in three-dimensional format; moreover, the electronic-density distribution profiles for these compounds were calculated using a “Gaussian’98” software [34].

Polarization resistance curves for the steel electrode in sulfuric acid in absence/presence of TCA and AcT, with different concentrations are shown in Fig. 4a and b, respectively. The corresponding electrochemical parameters for all the inhibitors using the polarization resistance measurements are given in Table 3. The data listed show that the inhibition efficiencies of different thiophene derivatives are still pronounced even at relatively low concentrations of the inhibitor used. However, the values of the inhibition efficiency increase with increasing concentration of sulfuric acid and as the con-

Table 3
Electrochemical parameters for stainless steel of type 316 in 0.5 M sulfuric acid solutions in absence and presence of different concentrations of 2-thiophene carboxylic acid (TCA)/2-acetyl thiophene (AcT)

Inhibitor (mol l^{-1})	E (mV)		β_c (mV decade^{-1})	β_a (mV decade^{-1})	R_p (10^2 Ω cm^2)	I_{corr} (10^{-4} A cm^{-2})	Corrosion rate (MPY)
	E_{oc}	E_{cor}					
0	−328/−328	−348/−348	88/88	55/55	1.64/1.64	0.90/0.90	82.5/82.5
5×10^{-4}	−396/−371	−414/−355	82/76	54/56	2.33/4.34	0.21/0.32	23.1/29.7
1×10^{-3}	−382/−392	−406/−369	81/94	47/49	3.41/7.22	0.13/0.19	11.6/17.8
5×10^{-3}	−404/−391	−418/−354	84/109	60/53	1.65/3.55	0.92/0.13	9.68/10.4
1×10^{-2}	−385/−382	−397/−373	78/71	56/77	6.89/19.4	0.62/0.080	5.77/7.39

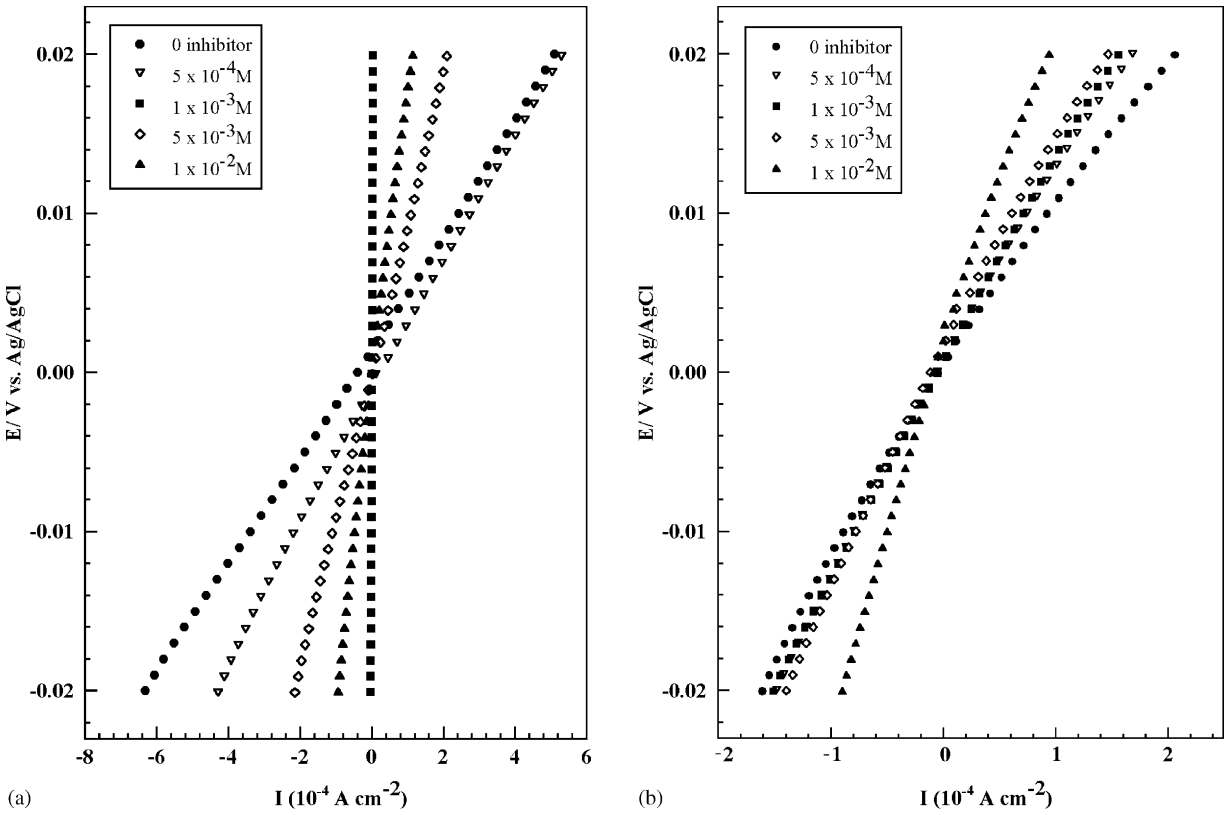

Fig. 4. Polarization resistance curves for the steel electrode in sulfuric acid in absence/presence of TCA (a) and AcT (b), with different concentrations.

centration of the inhibitor increases. The values of the anodic and cathodic Tafel constants (β_a and β_c), generally showed the same trend observed with TCH for the inhibitors studied. These values generally decrease upon addition of inhibitor and start to increase again in the case of AcT, showing irregularity after a critical concentration of the inhibitor is reached (ca. 1.0×10^{-3} M) [35]. It is recognized that the inhibitors that shift the entire current–potential curves towards more negative (cathodic) values are cathodic-type inhibitors while those that shift the curves in the anodic direction are anodic-type inhibitors [36]. On the other hand, mixed-type inhibitors cause a shift in the cathodic Tafel lines towards more negative values and the current–potential curves near the free corrosion potential towards less cathodic potentials. In this respect, the polarization results, namely for TCAL, TCH, and AcT, showed a shift of the entire potential–current curves towards more cathodic values upon addition of the inhibitor (cf. E_{corr} values in Tables 1–3). Moreover, the values of the anodic and cathodic Tafel constants decrease in the case of TCA and showed irregular values for AcT. Examination of Table 3 revealed that the polarization resistance increased dramatically upon the addition of the inhibitor and resulted in an increase in the slope of the polarization resistance curve upon increasing the concentration of the inhibitor in solution (cf. Fig. 4a and b). An inhibition efficiency of 99.3% was reached when using a concentration of 1.0×10^{-2} M of TCH. It is important to notice that a decrease in i_{corr} was observed upon addition of TCA that reached a limiting value at the concentration of 1.0×10^{-3} M, and started to increase as the concentration of TCA reached 1.0×10^{-2} M. The values of the anodic Tafel constant decreased from a value of 88.9 mV decade^{-1} for the uninhibited solution to a value of ≈50.0 mV decade^{-1} at higher concentrations of TCA. The corresponding values of the cathodic Tafel constant showed a change in value from 120.1 to around 88.0 mV decade^{-1}.

Corrosion rate calculations revealed that at the concentration of 1.0×10^{-3} M TCA, the minimal corrosion rate as well as maximum polarization resistance is achieved. This interesting observation could be explained on the basis that a critical concentration of TCA is reached in the solution that caused optimal inhibition efficiency for a particular concentration of the acid (cf. Fig. 5). Similar observations were cited earlier in the literature for other sulfur-containing compounds [37]. Above the optimal concentration, TCA eventually reduces rather than increases the inhibition efficiency. It was mentioned earlier that at low concentrations of sulfur-containing inhibitors, the surface coverage of the adsorbed molecules is too low to result in an efficient coverage to prevent corrosion of stainless steel [17]. Moreover, some authors [38,39] attributed this phenomenon to the hydrolysis of the sulfur compounds to produce corrosion-promoting species, such as HS^- and S^{2-}. Hydrolysis is only acceptable to take place in fairly concentrated solutions where the equilibrium constant of the protonated species of these compounds has to

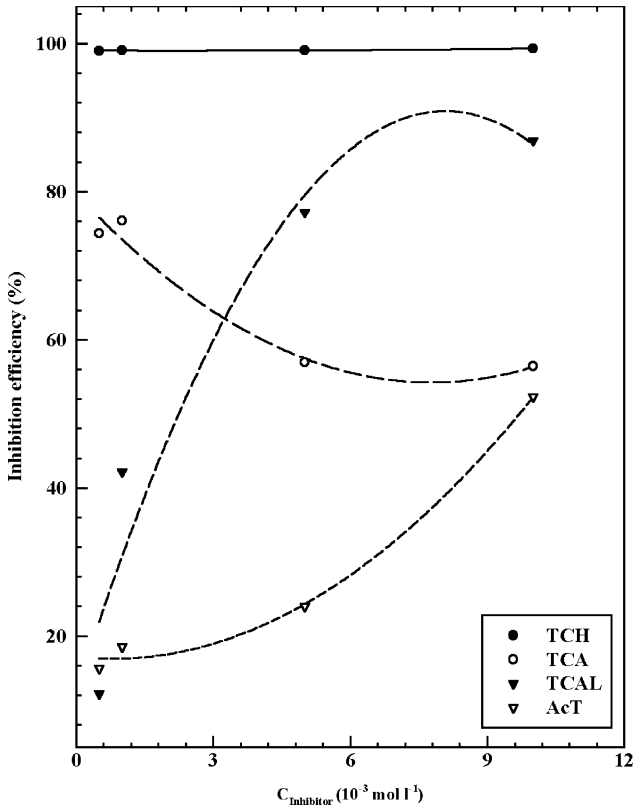

Fig. 5. Percentage inhibition efficiencies of thiophene derivatives with different concentrations for stainless steel in 0.5 M H_2SO_4.

be taken into account. Another likely mechanism for the observed results at this particular concentration of the inhibitor could be explained on the basis of increasing the acidity of solution via the carboxylic functionality of the inhibitor above a value of 1.0×10^{-3} M. Thus, exceeding this concentration of TCA results in two opposing effects, the first is increasing the inhibition efficiency and the second being the increase in the total acidity of the solution (cf. Fig. 5). Polarization resistance measurements data clearly exhibited an expected trend of increase in the slope of the potential–current curve with increase in the concentration of the inhibitor added. Tafel measurements (not shown) for stainless steel in sulfuric acid in absence and presence of different concentrations of AcT indicated, a shift in the anodic direction for the entire potential–current curves.

From the above discussion and the data shown in Fig. 5, the factors influencing the inhibition efficiency can be summarized as follows:

(i) The order of stability of the thiophene derivatives in solution and consequently their tendency to adsorb at the stainless steel surface.
(ii) The position of the substitution on the ring.
(iii) The number and nature of the substituent (degree of functionality).

Thus, the order of inhibition efficiency was TCH > TCAL ≅ TCA > AcT. The explanation of this order in reference to the above factors and molecular structure consideration could be as follows: the structure of the four thiophene derivatives posses a common part of the structure that is the thiophene moiety attached the C=O group. However, substitution in TCAL is at the 3-position when compared to the other inhibitors. The lone pairs on the two nitrogen atoms of TCH are delocalized and consequently will cause the structure to be stabilized. The stabilization energy resulted in the case of TCH in enhancing the surface coverage over the stainless steel through sulfur atoms anchoring around which the electron density is increased [38,39]. Therefore, the surface coverage in this case is expected to increase and results in an increase of the corrosion inhibition efficiency. A similar argument could be put forward in the case of TCA at relatively low concentrations. However, as the concentration of TCA increases in solution the local acidity at the surface of stainless steel increases. This later effect results in two competitive events, the first is inhibition through surface coverage and the second is enhancement to the dissolution (corrosion) at the initial stage of the anodic Tafel portion as indicated in the current–potential curve. The results indicated that TCAL exhibited a regular increase in the inhibition efficiency that reached a stable value at the higher concentration. The leveling in the inhibition efficiency could be explained by the formation of a thin polymeric layer at the surface of the stainless steel due to the polymerization of TCAL [40]. On the other hand, AcT exhibited the lowest inhibition efficiency. This could be explained in terms of the presence of the methyl group that affects the stability of the thiophene ring compared to the other derivatives.

3.6. Electrochemical impedance spectroscopy measurements

The corrosion behavior of stainless steel 316, in acidic solution in the presence of TCA and AcT with different concentrations was investigated by the electrochemical impedance spectroscopy measurements at room temperature. The locus of Nyquist plots is regarded as one part of a semicircle. The equivalent circuit model employed for this system is as previously reported in the literature [23] and shown in Fig. 6. Nyquist plots of stainless steel 316 in inhibited and uninhibited acidic solutions containing various concentrations of TCAL and AcT are shown in Fig. 7a and b. As could be noticed the impedance diagrams obtained are not perfect semicircles, and this could be attributed to frequency dispersion

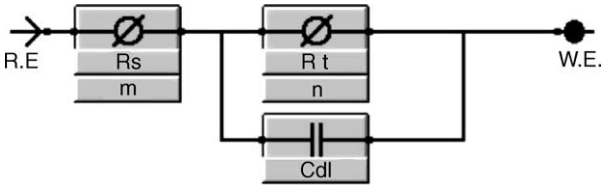

Fig. 6. Equivalent circuit used in the modeling of the electrochemical impedance spectroscopy data.

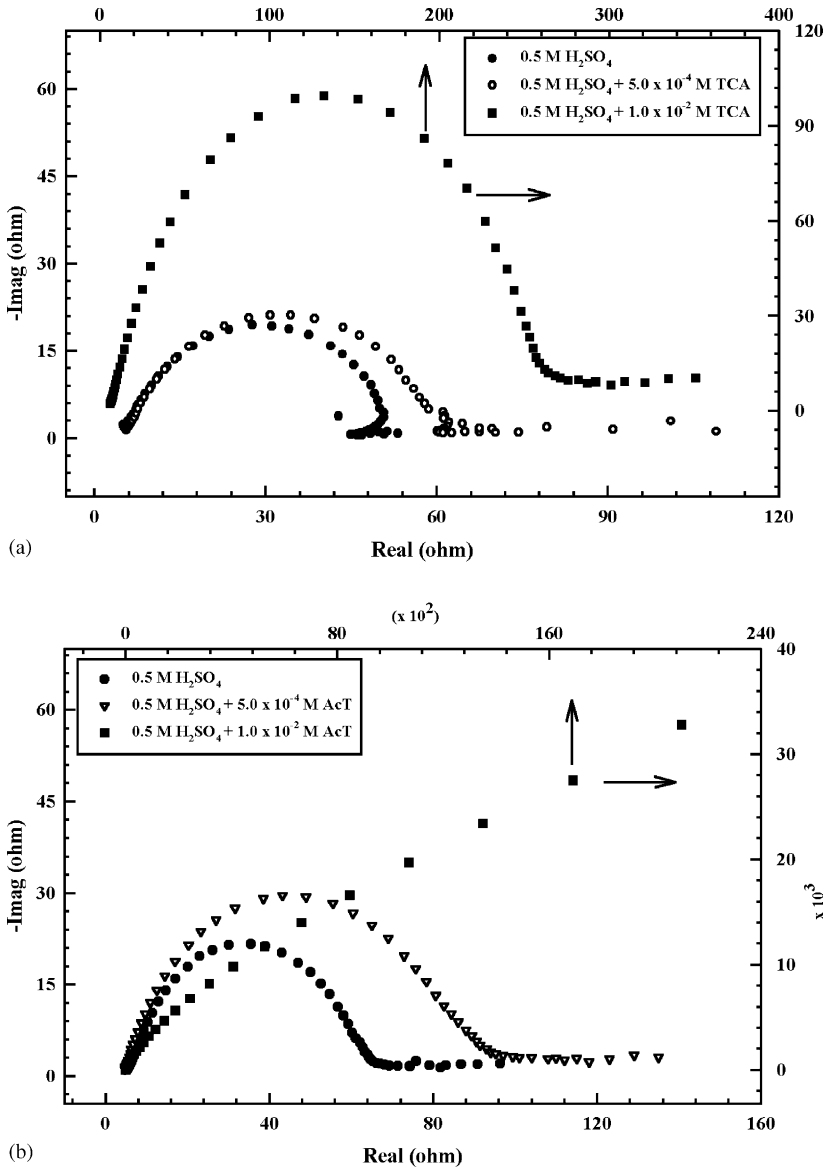

Fig. 7. Nyquist diagrams for stainless steel 316 in 0.5 M H_2SO_4 with different concentrations of TCA (a) and AcT (b).

as indicated earlier [41]. The charge transfer resistance, R_t, values could be calculated from the difference in impedance at lower and higher frequencies. To obtain the double layer capacitance (C_{dl}), the frequency at which the imaginary component of the impedance is maximum (−Imag max) is found and C_{dl} values could be calculated from the equation [41]:

$$f(-\text{Imag max}) = \frac{1}{2\pi C_{dl} R_{ct}} \quad (7)$$

It could be noticed from the data of Fig. 7a and b that the impedance semicircle size depends on the type and concentration of the inhibitor used. The presence of the semicircle in the impedance diagrams indicated that the corrosion of stainless steel 316 is controlled by a charge transfer process. Table 4 shows the impedance parameters obtained by line fitting to the semicircle. The charge transfer resistance (R_t) increases as the concentration of the inhibitor increases for the two inhibitors studied. Also, the double layer capacitance (C_{dl}) decreases with increase in the concentration of the inhibitor. This decrease is due to adsorption of inhibitor on the metal surface causing a change of the double layer structure as indicated earlier [42]. When comparing the inhibition efficiencies obtained from testing methods used in this study, it can be concluded that there is a fair agreement between our results and the results obtained by other techniques. Again, it could be noticed that TCA showed a higher inhibition efficiency when compared to AcT for the concentrations studied. In summary, all electrochemical techniques used in this study showed a comparable trend in the inhibition efficiency. The formation of a stable film through chemical/physical adsorption on the steel surface is responsible for the observed corrosion inhibition of the thiophene derivatives studied. It is

Table 4
AC impedance data for stainless steel of type 316 in 0.5 M H_2SO_4 in presence and absence of 2-thiophene carboxylic acid (TCA) and 2-acetyl thiophene (AcT)

Electrolyte (mol l^{-1})	R_t (10^2 Ω cm^{-2})	$1/R_t$ (10^{-2} Ω^{-1} cm^2)	C_{dl} (μF)	p
0 TCA	0.31	3.20	62.3	–
5×10^{-4} TCA	0.68	1.47	54.7	54.1
1×10^{-2} TCA	22	0.0460	45.0	85.6
0 AcT	0.31	3.20	62.3	–
5×10^{-4} AcT	0.53	1.89	41.3	40.9
1×10^{-2} AcT	1.0	0.98	18.6	69.4

worthwhile to mention that the inhibition efficiency was calculated from the measurements as indicated in Table 4 using the following relation [42]:

$$p = \frac{R_{t(uninh)}^{-1} - R_{t(inh)}^{-1}}{R_{t(uninh)}^{-1}} \quad (8)$$

where p is the inhibition efficiency, and $R_{t(uninh)}$ and $R_{t(inh)}$ are the charge transfer resistance values without and with inhibitor, respectively. We have followed the progress of R_t and C_{dl} with immersion time and noticed that without the inhibitor, R_{ct} decreases with immersion time, whereas C_{dl} increases. Both R_{ct} and C_{dl} change the trend to the opposite direction in presence of the inhibitor. It is possible to conclude that the change in R_{ct} and C_{dl} is due to the gradual replacement of water molecules on the metal surface, decreasing the extent of dissolution reaction.

4. Conclusions

Some thiophene derivatives can be used as inhibitors for the corrosion of stainless steel of type 316 in an acidic medium and in the presence of chloride ions. The inhibitors studied are considered as mixed-type inhibitors. The inhibition efficiencies are in the order of TCH > TCAL ≅ TCA > AcT. The substitution position on the thiophene ring, the stability of the thiophene cation-radical and the type of substituent affected the inhibition efficiency. A mechanistic explanation of the inhibition is attributed to the surface coverage of the organic molecule at the steel surface. The electrochemical impedance spectroscopy data fit to a Randel's circuit and the inhibition efficiency trend agrees well with DC measurements.

Acknowledgments

We are indebted to the partial financial support provided by the University of Cairo, the United Arab Emirates University and the University of Cincinnati.

References

[1] M.A. Streicher, in: R.Q. Barr (Ed.), Proceedings of the Symposium on Stainless Steels'77, Climax Molybdenum Co., Ann Arbor, 1977, p. 1.
[2] W.D. Binder, C.M. Brown, Proc. Am. Soc. Test. Mater. 46 (1946) 593.
[3] K.J. Bundy, Crit. Rev. Biomed. Eng. 22 (1994) 139.
[4] G. Schmitt, Br. Corros. J. 9 (1984) 165.
[5] B.A. Miksic, Magy. Kem. Lapja 46 (1991) 401.
[6] W.J. Lorentz, F. Mansfeld, Proceedings of the International Corrosion Conference Series 1988, NACE-7 (Corros. Inhib.), 1987, p. 7.
[7] N. Subramanyan, K. Ramkrishnaiha, S.V. Iyer, V. Kapali, Corros. Sci. 18 (1978) 1083.
[8] G. Trabanelli, Corrosion 47 (1991) 410.
[9] I. Sekine, T. Shimode, M. Yuasa, K. Takaoka, Ind. Eng. Chem. Res. 31 (1992) 434.
[10] R. Agrawal, T.K.G. Namboodhiri, J. Appl. Electrochem. 22 (1992) 383.
[11] A. Kumar, T. Singh, M.M. Singh, Trans. SAEST 27 (1992) 153.
[12] A. Kumar, M.M. Singh, Anti-Corros. Meth. Mater. 40 (1993) 4.
[13] V. Lvovich, A. Scheeline, Arch. Biochem. Biophys. 320 (1995) 1.
[14] A. Singh, R.S. Chaudhary, Br. Corros. J. 31 (1996) 300.
[15] G.O. Ilevbare, G.T. Burstein, Corros. Sci. 45 (2003) 1545.
[16] A.M. Al-Mayouf, A.K. Al-Ameery, A.A. Al-Suhybani, Corrosion 57 (2001) 614.
[17] X.L. Cheng, H.Y. Ma, S.H. Chen, R. Yu, X. Chen, Z.M. Yao, Corros. Sci. 41 (1999) 321.
[18] A. Kumar, S.P. Borthakur, H.C. Dhawan, Bull. Electrochem. (1999) 15.
[19] A. Singh, R.S. Chaudhary, Br. Corros. J. 31 (1996) 300.
[20] I. Marawi, A. Khaskelis, A. Galal, J.F. Rubinson, R.P. Popat, F.J. Boerio, H.B. Mark Jr., J. Electroanal. Chem. 434 (1997) 61.
[21] M. Kraljic, Z. Mandic, L. Duic, Corros. Sci. 45 (2003) 181.
[22] C. Gabrielli, Identification of Electrochemical Processes by Frequency Response Analysis (Monograph), Solartron Instrumentation Group, Hampshire, 1980, p. 53.
[23] F. Mansfeld, M.W. Kending, W.J. Lorenz, J. Electrochem. Soc. 132 (1985) 290.
[24] K.R. Threthewey, J. Chamberlain, Corrosion for Science and Engineering, second ed., Addison Wesley, Boston, 1995, 286.
[25] J.O'M. Bockris, D. Drasic, Electrochem. Acta 7 (1962) 293.
[26] M. Stern, L. Geary, J. Electrochem. Soc. 104 (1957) 56.
[27] X.L. Cheng, H.Y. Ma, S.H. Chen, X. Chen, Z.M. Yao, Corros. Sci. 41 (1999) 321.
[28] R. Agrawal, T.K.G. Namboodhiri, Corros. Sci. 30 (1990) 37.
[29] A. Attrens, B. Baroux, M. Mantel, J. Electrochem. Soc. 144 (1997) 3697.
[30] A. Galal, N.F. Atta, M.H.S. Al-Hassan, Mater. Chem. Phys., 2004, in press.
[31] F. Bentiss, M. Traisnel, M. Lagrence, Corros. Sci. 42 (2000) 127.
[32] M.A. Quraishi, M.A. Wajid Khan, S. Muralidharan, S. Venkatakrishna, J. Appl. Electrochem. 26 (1996) 1253.
[33] I. Singh, Corrosion 49 (1993) 473.
[34] J.B. Foresman, A. Frisch, Exploring Chemistry Electronic Structure Methods, Gaussian Inc., Pittsburgh, PA, 1996, p. 165.
[35] E.E. Ebenso, U.J. Ekpe, B.J. Ita, O.E. Offiong, U.J. Ibok, Mater. Chem. Phys. 60 (1999) 79.
[36] I.A. Ammar, F. El-Khorafi, Werkst. Korros. 12 (1973) 702.
[37] K. Pillai, R. Narayan, J. Electrochem. Soc. 125 (1978) 1393.

[38] A. Streitwieser Jr., Molecular Orbital Theory for Organic Chemists, Wiley, New York, 1961, p. 43.
[39] N. Hackerman, A.C. Makrides, Ind. Eng. Chem. 46 (1954) 523.
[40] R.D. McCullough, P.C. Ewbank, in: T.A. Skotheim, L. Elsenbaumer, J.R. Reynolds (Eds.), Handbook of Conducting Polymers, second ed., Marcel Dekker, New York, 1998, pp. 22–258.
[41] F. Mansfeld, M.W. Kending, S. Tsai, Corrosion 37 (1982) 301.
[42] Z. Szklarska-Smialowska, Electrochemical and Optical Techniques for the Study of Metallic Corrosion, Kluwer Academic Publishers, Dordrecht, 1991, p. 545.